Conformal map modeling of the pinning transition in Laplacian growth

H. G. E Hentschel,[1] M. N. Popescu,[2] and F. Family[1]
[1]*Department of Physics, Emory University, Atlanta, Georgia 30322*
[2]*Max-Planck-Institute für Metallforschung, Heisenbergstrasse 1, D-70569 Stuttgart, Germany*
(Received 14 October 2001; published 6 March 2002)

In Laplacian growth processes pinning may be expected due to a nonlinear response of a material during dielectric breakdown, or due to stick-slip boundary conditions in two-fluid flow in a porous medium, while thermal noise will lead to depinning. Using a method recently proposed by Hastings and Levitov, the size $R_{max} \sim E_c^{-\alpha}$ of the pinned pattern is shown to scale with the critical field E_c (electric field for dielectric breakdown, pressure gradient for fluid flow). These pinned patterns have a lower effective fractal dimension d_f than diffusion-limited aggregation due to the enhancement of growth at the hot tips of the developing pattern. At finite temperature, thermal noise leads to depinning and growth of patterns with a shape and dimensionality dependent on both E_c and the thermal noise. Using multifractal analysis, scaling expressions are established for this dependency.

DOI: 10.1103/PhysRevE.65.036141 PACS number(s): 02.50.−r, 61.43.Hv, 77.22.Jp, 45.70.Qj

I. INTRODUCTION

The importance of diffusion-limited aggregation (DLA) as a paradigm for nonequilibrium growth and pattern formation has constantly increased in the twenty years since its discovery by Witten and Sander [1]. The reason is multifold. First, it is a self-organized growth process leading naturally to fractal structures. Second, it has been identified as a stripped down model for several physical processes such as dielectric breakdown [2], electrochemical deposition [3,4], and two-fluid Laplacian flow [5]. Although we have gained a great deal of understanding of DLA during this period, many important questions remain open. One such issue is the influence on the type of pattern formed of a critical threshold E_c in the electric field for dielectric breakdown, or equivalently of a critical pressure gradient for flow to occur as the fluid-fluid phase boundary wanders inside a porous medium. This question is important for both practical reasons in increasing our understanding of real dielectric breakdown and two-fluid flow in porous media, and theoretically because still little is known about how the self-similar multifractal structure of DLA emerges.

As far as dielectric breakdown is concerned, the basic argument putting it in the same universality class as DLA involves the assumption that the probability of dielectric breakdown is proportional to the electric field (or, in the generalized models [2], to the local electric field to some power η, i.e., E^{η}). Though this dielectric breakdown model is very useful from a theoretical viewpoint in discussing fractal growth processes, it is unlikely to represent the physics of sparking in a real material. The simplest model that might describe this phenomenon would be to introduce a material dependent critical electric field E_c for breakdown to occur.

Similar constraints can be identified in the context of two-fluid immiscible flow in in a porous medium. A Saffmann-Taylor instability is known to exist [6] and DLA has been identified as the appropriate universality class for the fractal structure formed by this type of Laplacian flow [5]. Such a fluid-fluid phase boundary wanders in a highly disordered medium in which the less viscous fluid is nonwetting (in two dimensions, think of a Hele-Shaw cell filled with porous material whose pores are saturated with a viscous oil that is being displaced by a nonwetting low viscosity water). Thus, one would expect the pressure gradient at the interface above to have a critical value for flow $|\nabla p| > E_c \sim \sigma/\kappa$, where σ is the effective surface tension of the water in the pores and κ is the permeability of the porous medium.

These two physical situations in which a similar material dependent critical parameter E_c naturally occurs then raise the question as to how this criticality influences the growth and form of the pattern. In this paper we show that such a threshold for growth has remarkable consequences: its influence is crucial to both growth—the patterns ultimately all become pinned and to form—the rich branched stucture of DLA is replaced by a much lower-dimensional shape consisting of a few surviving branches that are the last to be pinned.

Since in this paper we are addressing Laplacian flows, we will make use of a powerful tool recently proposed by Hastings and Levitov [7,8], namely, iterated conformal mapping. It has been already shown that DLA in two dimensions can be grown by iterating stochastic conformal maps, and we will show that a simple variant of this method allows us to study Laplacian growth in the presence of a critical field.

Therefore, in Sec. II we introduce the model we wish to study using iterated conformal maps. In Sec. III, we describe how physical properties of the growth pattern are extracted from the developing conformal map. In Sec. IV, we study the scaling properties exhibited by such patterns when pinned, and estimate the dependence of the pinning exponents on E_c as well as the fractal dimension of the pinned clusters. In Sec. V, we study the scaling behavior of the first Laurent coefficient of the mapping (which is proportional to the cluster radius) near the pinning. In Sec. VI, we examine the influence of thermal noise on depinning, and we conclude with a discussion of the results in Sec. VII.

II. CONFORMAL MODELING OF LAPLACIAN GROWTH WITH CRITICAL GRADIENTS

A simple physical model for studying the time development of pinning in Laplacian growth is therefore to assume

that the pressure gradient $\nabla p(s)$ (we shall use the language of two-fluid flow in most of this paper though naturally we might equally have used the electric field $E(s)$ in the language of dielectric breakdown) at a point s on the developing interface should be greater than a certain critical value E_c, in order for motion of the interface to occur at a point s on the interface. Thus, the normal velocity $\mathbf{v}(s)$ of the interface will be given by

$$\mathbf{v}(s)=\begin{cases} -\kappa\nabla p & \text{if } |\nabla p|>E_c, \\ 0 & \text{if } |\nabla p|<E_c. \end{cases} \tag{1}$$

If the flows are incompressible then the pressure field outside the developing pattern will still obey Laplace's equation $\nabla^2 p=0$, and consequently the extremely difficult problem of calculating the pressure field in the presence of the constant pressure boundary conditions on the freely evolving interface can be handled by using conformal mapping techniques.

The basic idea is to follow the evolution of the conformal mapping $\Phi^{(n)}(w)$ that maps the exterior of the unit circle in a mathematical w plane onto the complement of the cluster of n particles in the physical z plane. $\Phi^{(n)}(w)$ is unique by the Riemann mapping theorem, given that it satisfies the boundary condition

$$\Phi^{(n)}(w)\sim F_1^{(n)} w \quad \text{as} \quad w\to\infty, \tag{2}$$

where $F_1^{(n)}$ is the first Laurent coefficient in the expansion of the mapping, a real positive coefficient, fixing the argument of $[\Phi^{(n)}(w)]'$ to be zero at infinity.

As the complex pressure in the mathematical plane obeys $\Psi^{(n)}(w)=p+i\psi=\ln w$ (we assume the pressure on the free boundary $|w|=1$ of the flow to obey $p=0$), the complex pressure $\Psi^{(n)}(z)$ in the physical plane is given by

$$\Psi^{(n)}(z)=\ln[\Phi^{(n)}]^{-1}(z), \tag{3}$$

where $[\Phi^{(n)}]^{-1}(z)$ is the inverse mapping and automatically satisfies $p(s)=0$ on the free boundary of the flow. Assuming $z\to\infty$ in Eq. (2), it is easy to verify that Eq. (3) implies

$$\Psi^{(n)}(z)\sim \ln z \quad \text{when} \quad z\to\infty, \tag{4}$$

as it should be in two dimensions.

The equation of motion for $\Phi^{(n)}(w)$ is determined recursively (see Fig. 1). The choice of the initial map $\Phi^{(0)}(w)$ is rather flexible, and in this paper we select (arbitrarily) an initial condition $\Phi^{(0)}(w)=w$ since we expect the asymptotic cluster to be independent of this choice. Assuming that $\Phi^{(n-1)}(w)$ is given, then the cluster of n ''particles'' is created by adding a new ''particle'' of constant shape and linear scale $\sqrt{\lambda_0}$ to the cluster of $(n-1)$ ''particles'' at a position that is chosen randomly according to the harmonic measure, provided the pressure gradient obeys Eq. (1), $|\nabla p|>E_c$. How is this constraint achieved?

We denote points on the boundary of the cluster by $z(s)$, where s is an arc-length parametrization. Using Eq. (3), one has $|\nabla p|=|d\Psi^{(n)}/ds|=1/|d\Phi^{(n)}/dw|$, and therefore the probability to add a particle on an infinitesimal arc ds centered at the point $z(s)$ on the cluster boundary is

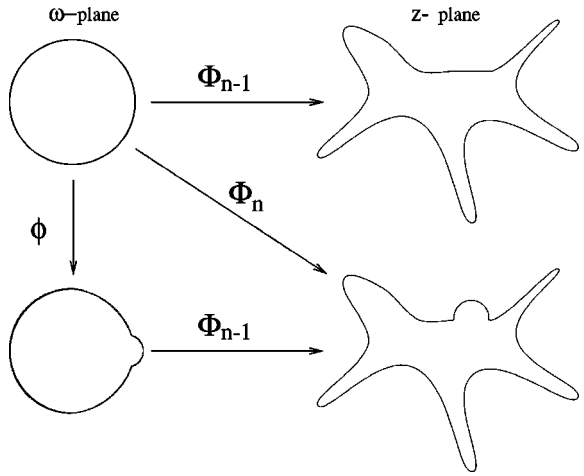

FIG. 1. Diagramatic representation of the mappings Φ and ϕ.

$$P(s,ds)\sim|d\Psi(s)/ds|ds. \tag{5}$$

The preimages of $z(s)$ and ds in the w plane being $e^{i\theta}$ and $d\theta$, respectively, it follows that $ds=|[\Phi^{(n-1)}]'(e^{i\theta})|d\theta$, and we therefore conclude that

$$P(s,ds)=|d\Psi(s)/ds||\Phi'|d\theta=d\theta. \tag{6}$$

Thus, the harmonic measure on the real cluster translates to a uniform measure on the unit circle in the mathematical plane, and all we need for fulfilling the constraint is to grow only at values of θ that obey

$$1/|[\Phi^{(n-1)}]'(e^{i\theta})|>E_c. \tag{7}$$

Let us define now a new function $\phi_{\lambda_n,\theta_n}(w)$. This function maps the unit circle to the unit circle with a bump of linear scale $\sqrt{\lambda_n}$ around the point $e^{i\theta_n}$. For $w\to\infty$, $\phi_{\lambda_n,\theta_n}(w)\sim w$ (with positive real proportionality coefficient). Using $\phi_{\lambda_n,\theta_n}(w)$ the recursion relation for $\Phi^{(n)}(w)$ is given by (see Fig. 1)

$$\Phi^{(n)}(w)=\Phi^{(n-1)}(\phi_{\lambda_n,\theta_n}(w)). \tag{8}$$

so the right-hand side of Eq. (8) is determined completely by $\Phi^{(n-1)}(w)$, and the Eq. (8) induces the recursive dynamics of $\Phi^{(n)}(w)$.

Finally, to close the set of equations λ_n must be chosen to obey

$$\lambda_n=\frac{\lambda_0}{|\Phi^{(n-1)\prime}(e^{i\theta_n})|^2} \tag{9}$$

in order to ensure that a bump of size $\sqrt{\lambda_0}$ is added in the physical z plane.

The recursive dynamics can be represented as iterations of the elementary bump map $\phi_{\lambda_n,\theta_n}(w)$,

$$\Phi^{(n)}(w)=\phi_{\lambda_1,\theta_1}\circ\phi_{\lambda_2,\theta_2}\circ\cdots\circ\phi_{\lambda_n,\theta_n}(\omega). \tag{10}$$

Although this composition appears at first sight to be a standard iteration of stochastic maps, this is not so because the order of iterations is inverted—the last point of the trajectory is the inner argument in this iteration. As a result the transition from $\Phi^{(n)}(w)$ to $\Phi^{(n+1)}(w)$ is not achieved by one additional iteration, but by composing the n former maps Eq. (10) starting from a different seed that is no longer ω but $\phi_{\lambda_{n+1},\theta_{n+1}}(w)$.

There is a certain freedom in choosing the nonunique function $\phi_{\lambda,\theta}$ that conformally maps the unit circle to the unit circle with a bump. An optimal choice for $\phi_{\lambda_n,\theta_n}(w)$ that ensures that the bump is localized has been proposed in Ref. [7] and is given by

$$\phi_{\lambda,0}(w)=w^{1-a}\left\{\frac{(1+\lambda)}{2w}(1+w)\left[1+w+w\left(1+\frac{1}{w^2}-\frac{2}{w}\frac{1-\lambda}{1+\lambda}\right)^{1/2}\right]-1\right\}^{a}, \tag{11}$$

$$\phi_{\lambda,\theta}(w)=e^{i\theta}\phi_{\lambda,0}(e^{-i\theta}w), \tag{12}$$

where the parameter a is confined to the range $0<a<1$. As a decreases the bump becomes flatter, with the identity map obtained for $a=0$. As a increases towards unity the bump becomes elongated normally to the unit circle, with a limit of becoming a line (''strike'' in the language of Ref. [7]) when $a=1$. Following the analysis in Ref. [9], we have used $a=0.66$ througout this paper, as we believe the large scale asymptotic properties will not be affected by the microscopic shape of the added bump.

III. ALGORITHM AND EXTRACTION OF CLUSTER PROPERTIES

The algorithm simulating the growth of the cluster is based on Ref. [9]. The n-''particle'' cluster is encoded by the series of pairs $\{(\theta_i,\lambda_i)\}_{i=1}^{n}$. Having the first $n-1$ pairs, the nth pair is found as follows: choose θ_n from a uniform distribution in $[0,2\pi]$, independent of previous history. If it obeys the constraint given by Eq. (7) accept this value of θ_n, otherwise repeat until the constraint is obeyed. If no acceptable value of θ_n is found after a given number of attempts $m(n)$ (see also Sec. IV where the attempt algorithm is discussed in greater detail) the cluster is assumed to be pinned. Otherwise, we compute λ_n from Eq. (9), where the derivative of the iterated function $\Phi^{(n-1)}$ involves $\phi'_{\lambda_{n-1},\theta_{n-1}}$, $\phi'_{\lambda_{n-2},\theta_{n-2}}$, $\phi'_{\lambda_{n-3},\theta_{n-3}}$, etc, computed, respectively, at the points $e^{i\theta_n}, \phi_{\lambda_{n-1},\theta_{n-1}}(e^{i\theta_n}), \phi_{\lambda_{n-2},\theta_{n-2}}[\phi_{\lambda_{n-1},\theta_{n-1}}(e^{i\theta_n})]$, etc. Note that the evaluation of both ϕ' and ϕ after the addition of one particle involves $O(n)$ operations since the seed changes at every n, and this translates into $n^2m(n)$ time complexity for the growth of an n-particle cluster.

Once the mapping $\Phi^{(n)}(w)$ has been found, essentially all questions of physical interest can be addressed. For example, the local pressure gradient is given by the derivative of the mapping $|\nabla p|=1/|\Phi^{(n-1)'}(e^{i\theta_n})|$, while the radius of the developing pattern can be extracted from the first Laurent coefficient $F_1^{(n)}$ of the mapping.

To see how this occurs we start with the observation that since the functions $\Phi^{(n)}(w)$ and $\phi_{\lambda,\theta}(w)$ are required to be linear in w at infinity, they can be expanded in a Laurent series in which the highest power is w,

$$\Phi^{(n)}(w)=F_1^{(n)}w+F_0^{(n)}+F_{-1}^{(n)}w^{-1}+F_{-2}^{(n)}w^{-2}+\cdots, \tag{13}$$

$$\phi_{\lambda,\theta}(w)=f_1w+f_0+f_{-1}w^{-1}+f_{-2}w^{-2}+\cdots, \tag{14}$$

where

$$f_1=(1+\lambda)^a,$$

$$f_0=\frac{2a\lambda e^{i\theta}}{(1+\lambda)^{1-a}},$$

$$f_{-1}=\frac{2a\lambda\, e^{2i\theta}}{(1+\lambda)^{2-a}}\left(1+\frac{2a-1}{2}\lambda\right),$$

$$f_{-2}=\frac{2a\lambda e^{3i\theta}}{(1+\lambda)^{3-a}}\left(1+2(a-1)\lambda+\frac{2a^2-3a+1}{3}\lambda^2\right).$$

Thus the recursion equations for the Laurent coefficients of $\Phi^{(n)}(w)$ can be obtained by substituting the series of Φ and ϕ into the recursion formula (8). Specifically,

$$F_1^{(n)}=F_1^{(n-1)}f_1^{(n)}=\prod_{i=1}^{n}(1+\lambda_i)^a, \tag{15}$$

and therefore given the set of $\{\lambda_i\}$ we can calculate $F_1^{(n)}$.

Furthermore, from the one-fourth theorem [9], which states that the interior of the curve $\{z:z=\Phi^{(n)}(e^{i\theta})\}$ is contained in a circle of radius $4F_1^{(n)}$, follows that $F_1^{(n)}$ is a typical length scale of the cluster and thus a natural choice for the radius of the cluster is $R\simeq F_1^{(n)}$. As any typical radius of the cluster should scale like $n^{1/D}\sqrt{\lambda_0}$, where D is the dimension of the cluster, we can thus expect $F_1^{(n)}$ to scale as

$$F_1^{(n)}\sim n^{1/D}\sqrt{\lambda_0}. \tag{16}$$

We note in passing that this scaling law was used in Ref. [9] as a very convenient way to measure the fractal dimension of the growing cluster.

IV. THE PINNING TRANSITION IN LAPLACIAN GROWTH

The existence of a critical pressure gradient E_c for flow or dieletric breakdown automatically means that all growth patterns will ultimately become pinned in the absence of noise because the pressure gradients diminish in a power law multifractal fashion as the cluster grows [10–12]. For example, for a two-dimensional compact flow we would expect $|\nabla p(s)|\sim 1/R$, where R is the radius of the growing cluster, while for a fractal shape multifractal theory shows that even the stron-

gest gradients scale as $|\nabla p(s)| \leqslant 1/R^{D_\infty}$, which also tends asymptotically to zero.

The actual manner in which the cluster will be pinned can be extracted by studying pinning as a function of E_c. We note, however, that the definition of a ''pinned'' cluster is an important question that needs to be dealt with in our algorithm. In principal, one should test each possible growth site that means making $m(N) \sim N$ attempts to continue growth of the N-particle cluster before accepting the cluster as pinned. In practice, this means a drastic slowing down of the whole algorithm, which becomes a $O(N^3)$ and only small clusters can be grown in a reasonable amount of time. On the other hand, one may argue that if the hottest tips (which are visited every $\sim N^{D_\infty/D}$ steps) do not grow, then the whole cluster will be pinned. Assuming this as definition of ''pinned,'' the whole algorithm can be reduced to $O(N^{2+D_\infty/D})$ allowing reasonably large clusters to be grown. In practice, we find that while at given E_c the ''pinned'' clusters are (not surprisingly) smaller in the second case, the scaling behavior that we find is unaffected. This can be seen in our results for both the scaling of the pinned cluster radius R_c with critical pressure gradient for flow E_c and the scaling of the pinned cluster size N_c with critical pressure gradient for flow E_c (see Fig. 2).

Summarizing the results of our simulations, we note that the pinned cluster radius and size both scale with E_c. The maximal radius of the pattern scales as

$$R_c \sim E_c^{-\alpha} \tag{17}$$

with $1.6 < \alpha < 1.8$, while the maximal size of the pattern scales as

$$N_c \sim E_c^{-\beta} \tag{18}$$

with $\beta \approx 2.25$.

In consequence, the pinned pattern retains mass-radius scaling [see Fig. 2(c)] as N_c scales with R_c as

$$N_c \sim R_c^{d_f} \tag{19}$$

with $1.25 < d_f = \beta/\alpha < 1.4$, although the resulting pattern no longer possesses local self-similarity, and thus is not a fractal.

How can we understand these results? From multifractal scaling [11,12] we know that the interface of the cluster consists of sets of $N_\alpha \sim (R/\sqrt{\lambda_0})^{f(\alpha)}$ sites with pressure gradients $|\nabla p| \sim (R/\sqrt{\lambda_0})^{-\alpha}$. Thus, we would expect that the weakest gradients, normally deep in the fjords, would be pinned first, with the hot tips surviving longest, and indeed this is what is observed in simulations, as shown in Fig. 3. The two clusters correspond to DLA with $E_c = 0$, and to a cluster grown with a pinning gradient $E_c = 0.002$, and one can see that deep inside the cluster the DLA grows further than the pinned cluster, while the hot tips of the pinned cluster are more likely to grow than in DLA. The same effect can be seen in the development of the first Laurent coefficient $F_1^{(n)}$ before pinning occurs (see Fig. 4).

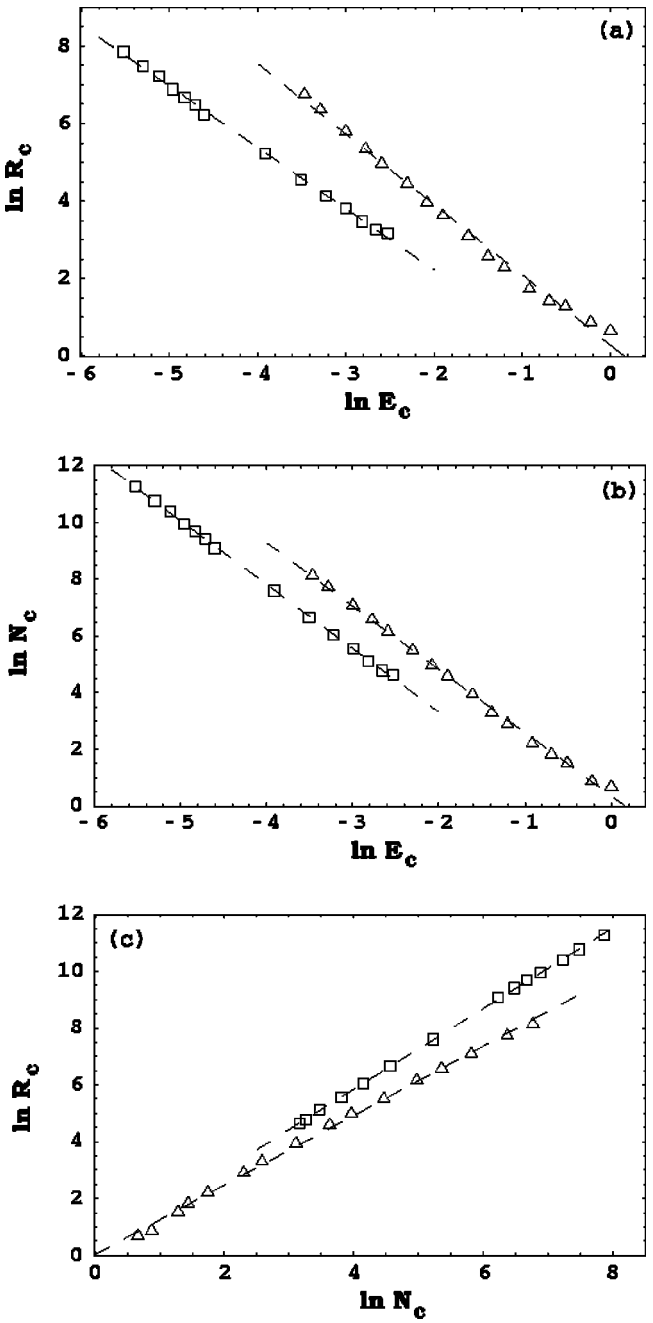

FIG. 2. Scaling of the pinned cluster: (a) radius R_c with critical pressure gradient for flow E_c; (b) size N_c with critical pressure gradient for flow E_c; (c) size N_c with radius R_c. Triangles, $m(N) \sim N$ attempts before pinning; squares, $m(N) \sim N^{D_\infty/D}$. The dashed lines are linear fits to the data.

In order to understand these results theoretically let us begin with a very simplistic argument that will help to set the stage for a better estimate. As we mentioned, one would expect the hot tips to have the maximal growing probability and thus to be pinned last. These maximal growth probabilities in DLA scale as $D_\infty = D - 1$ (where $D \approx 1.713$ is the fractal dimension for DLA, and we have assumed the Sher-Turkovitch identity [13] to be valid). Therefore, as a first estimate we assume the clusters are pinned when $P_{max} \sim (\sqrt{\lambda_0}/R_{max})^{D_\infty} \sim E_c$. Before pinning we shall assume that

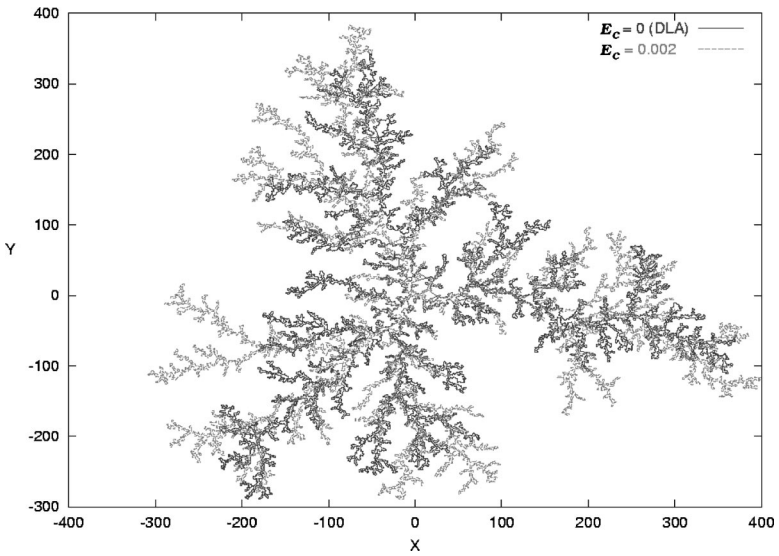

FIG. 3. Two clusters grown with the same set of random numbers. (i) A DLA cluster; (ii) a cluster where $E_c = 0.002$. Note both the pinned regions deep in the cluster and hot tips that grow preferentially.

the cluster scales like DLA and therefore $N_{max} \sim R_{max}^D$. If both these assumptions were correct, we would then find that

$$\alpha = 1/D_\infty \approx 1.4, \tag{20}$$

$$\beta = D/D_\infty \approx 2.4, \tag{21}$$

$$d_f = D \approx 1.7. \tag{22}$$

But we know that this argument is not quite correct because the growing prepinned cluster is not in the same universality class as DLA, and probably it is not even a fractal object. As can be seen in Fig. 4, the first Laurent coefficient shows that there is a breakdown in scaling after an initial period when DLA scaling $F_1^{(n)} \sim n^{1/D}$ applies.

A better estimate therefore is to start with the question about when will the influence of E_c make itself felt and cause crossover to a new growth mode? Based on the fact that essentially all the measure in a harmonic fractal (the integral over the electric field in the case of dielectric breakdown, or the pressure gradient in the case of two-fluid flow) lies on a one-dimensional interface $D_1 = 1$, one would expect crossover at scales l when $P_{information} \sim (\sqrt{\lambda_0}/l) \sim E_c$. Thus, instead of a DLA-like structure on all scales, a description of the cluster more likely to be correct is that it remains fractal on scales $r \ll l$ but becomes linear on scales $r \gg l$. If this description is valid, then

$$\beta = \alpha + (D-1). \tag{23}$$

Retaining our estimate of β (which was based on the fact that pinning can be expected when the hot tips can no longer grow), we find

$$\alpha = D/D_\infty - (D-1) \approx 1.7, \tag{24}$$

$$\beta = D/D_\infty \approx 2.4, \tag{25}$$

$$d_f = \beta/\alpha \approx 1.3, \tag{26}$$

in good agreement with simulations.

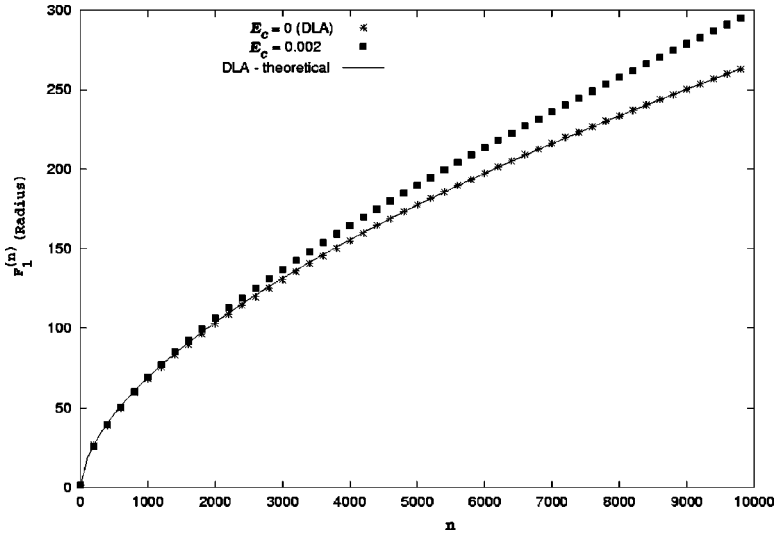

FIG. 4. Time development of the first Laurent coefficient $F_1^{(n)}$ for two clusters. (i) A DLA cluster; (ii) a cluster where $E_c = 0.002$. The solid line shows the theoretical DLA behavior $F_1^{(n)} \sim n^{(1/D)}$. Note how for the same value of n the pinned cluster typically has a larger radius due to the hot tips that grow preferentially.

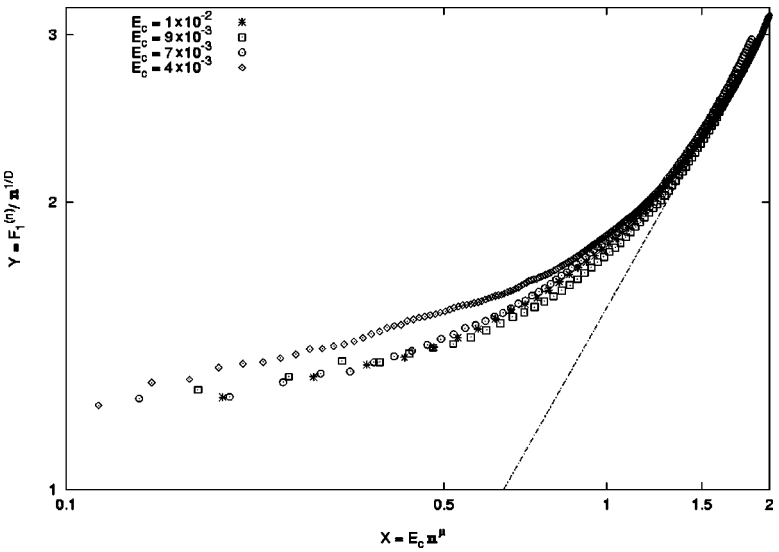

FIG. 5. Data collapse of $F_1^{(n)}(E_c)/n^{1/D}$ plotted against $E_c n^{\mu}$. The asymptotic form $f(x)\to x$ is shown for purposes of comparison. The value μ leading to the best data collapse is $\mu\simeq 0.55$.

V. SCALING IN THE PREPINNING REGIME

It is possible to go further theoretically and derive a scaling form for the first Laurent coefficient $F_1^{(n)}$ of the mapping before pinning occurs. This scaling form is based on the following observation. It appears that the evolving pattern is asymptotically forming the maximally branched structure subject to the constraint that only sites with a pressure gradient $|\nabla p|>E_c$ can grow. Using for the moment the language of electrostatics, the integral of the electric field around the pattern $\int_0^L E(s)ds$ (which is the total flux) is equal to the charge on the object and is conserved during growth. The maximally branched object (just before pinning occurs) would thus consist of $N_{growth}\sim 1/E_c$ hot tips each with a growth probability $P_{growth}\sim E_c$. Such an asymptotic flow pattern would scale as $(R/\sqrt{\lambda_0})\sim E_c N$, and this leads to the following scaling form for the first Laurent coefficient:

$$F_1^{(n)}(E_c)=n^{1/D}\sqrt{\lambda_0}f(E_c n^{\mu}). \tag{27}$$

Since the initial behavior is DLA-like and therefore

$$f(x)\to f(0) \quad \text{as } x\to 0, \tag{28}$$

while the final growth is linear $F_1^{(n)}(E_c)\sim E_c n$ and therefore

$$f(x)\to x \quad \text{as } x\to\infty \tag{29}$$

it then follows that $\mu=(D-1)/D\approx 0.416$.

To check this prediction, in Fig. 5 we have plotted $F_1^{(n)}(E_c)/n^{1/D}$ against $E_c n^{\mu}$, and as can be seen all the data collapse with the scaling function $f(x)$ having the form given by Eqs. (28) and (29).

VI. THE INFLUENCE OF NOISE ON DEPINNING

So far we have assumed that there exists a critical value E_c of the electric field or pressure gradient for growth to occur and therefore all patterns are ultimately pinned. In the presence of thermal noise, as will be the case in most physical situations, depinning can occur and thus the pinned patterns will represent the $T=0$ limit of a finite temperature phase diagram, while DLA will be the $T\to\infty$ limit. To generate nonzero temperature patterns, we can use a variation of a Monte Carlo algorithm in which the probability for growth at a site s is $P(s)=\min\{1,\exp[\beta(|\nabla p|-E_c)]\}$, where $\beta=1/T$. In the conformal mapping approach, this translates to a variation of Eq. (7), i.e., the probability of growth at the randomly chosen point θ on the unit circle will be given by

$$P(\theta)=\min\{1,\exp[\beta(1/|[\Phi^{(n-1)}]'(e^{i\theta})|-E_c)]\}. \tag{30}$$

The types of clusters corresponding to this type of growth can be seen in Fig. 6.

Numerical simulations with fixed critical E_c and increasing temperature (decreasing β) reveal that the fractal dimension of the resulting clusters appear to depend continuously on βE_c. That is scaling behavior $F_1^{(n)}\sim n^{1/D(\beta E_c)}$ is observed for all β and E_c, as illustrated in Fig. 7.

We would like to emphasize two points. First, as must be the case for high temperature, DLA patterns appear and therefore $D\to D_{DLA}$ when $\beta E_c\ll 1$. Second, the fractal dimension reduces continuously, apparently reaching $D=1$ for a finite value of $\beta E_c\approx 3.5$, thus implying a transition to pure one-dimensional growth at finite, nonzero temperature. This last result is tentative as is the suggestion that the fractal dimension depends only on the product βE_c, and further work with different parameters is required before a clear conclusion can be drawn.

VII. SUMMARY AND DISCUSSION

In this paper, we have shown numerical evidence that a threshold for growth dramatically influences both the growth pattern and the form of the cluster. Scaling relations for the pinned patterns have been proposed based on numerical evidence, and the scaling exponents of the pinned cluster have been derived as well as the form of the mass-radius scaling in the prepinning regime.

We expect that simple extentions of this model may be important in other domains of physics. For example, in the

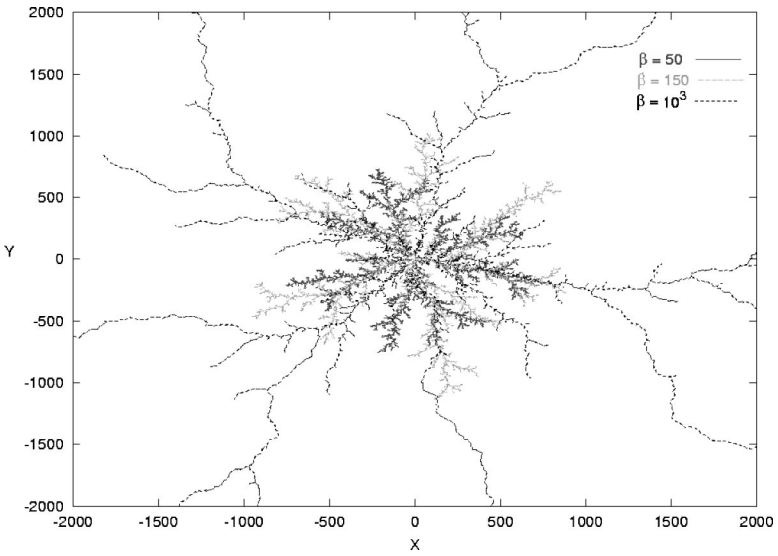

FIG. 6. Cluster growth in the presence of noise. All have $E_c=0.01$. The values of the effective inverse temperature $\beta=1/T$ are, respectively, (i) $\beta=50$; (ii) $\beta=150$; (iii) $\beta=1000$. Note the transition from a branched DLA structure as $T\rightarrow\infty$ to a few rivulets or arcs as $T\rightarrow 0$.

presence of applied shear viscoelastic behavior is exhibited by thin films, an initial elastic behavior being followed, at a well-defined yield stress, by shear melting and ductile flow [14,15]. This observed stick-slip behavior is not only due to the ordered state of the thin film of fluid but also to the presence of velocity weakening boundary conditions at the mesoscale. These significantly modify the lubricating properties of thin films creating localized mesoscopic regions of stick and slip in the sheared film [16], and how the flow patterns change due to such stick-slip boundary conditions can be studied using an approach similar to the one presented here.

Also, we note that the patterns created by a wandering contact line may also lie in a related universality class. During wetting of a surface by a droplet, any volatility or contamination in the wetting fluid will lead to temperature and surface-tension gradients resulting in additional forces (the Marangoni effect). The alteration in dynamics may be dramatic: for example, if surfactant solutions are spread on moist surfaces large surface-tension gradients will appear leading to a fingering of the contact line [17], and the spreading is an order of magnitude faster than surface tension or gravity dominated wetting. Since such gradients are easily accomodated in the present method, in principle, one could obtain in this manner evidence on whether the universality class is the same or not.

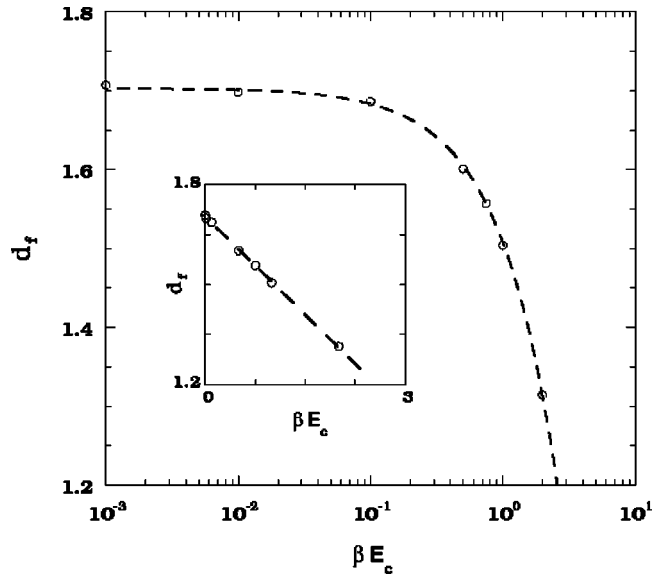

FIG. 7. Mass-radius scaling exponent d_f as a function of βE_c at $E_c=0.01$ (semilog plot, respectively, linear plot in the inset). Numerical evidence suggests there may be a transition to one-dimensional structures at finite values of $\beta E_c\approx 3.5$. A fit to the data (solid line) suggests that d_f depends linearly on βE_c.

Finally, we have to emphasize the fact that the results presented in this paper raise and leave open a number of questions about the influence of material properties and noise on Laplacian growth patterns and suggest that one is unlikely to achieve a good understanding of DLA in isolation from a parameter space incorporating these parameters. Some of these questions would include: Is the fractal dimension truely a function of only βE_c? Is there a phase transition at a finite value of βE_c to one-dimensional (but finitely branched clusters) as suggested above? We expect the answers to these question to involve a detailed study of the effect of E_c and β on the multifractal distribution of the cluster.

There is another important point that we have not mentioned in this paper but could have a profound effect on the growth pattern. That is whether the cluster is grown serially (as we have done here or in pure DLA) or in parallel (as the algorithm for Laplacian flows would suggest from its continuum descrition). Very recently iterated conformal mapping methods have been used to study this question [18], and it appears that Laplacian growth and DLA may lie in different universality classes. This is an important question for future study.

ACKNOWLEDGMENTS

Acknowledgment is made to the donors of The Petroleum Research Fund, administered by the ACS, for support of this research. We would also like to thank L. Sander and M. Hastings for useful comments made during this work.

[1] T.A. Witten, Jr. and L.M. Sander, Phys. Rev. Lett. **47**, 1400 (1981).
[2] L. Niemeyer, L. Pietronero, and H.J. Wiesmann, Phys. Rev. Lett. **52**, 1033 (1984).
[3] R.M. Brady and R.C. Ball, Nature (London) **309**, 225 (1984).
[4] M. Matsushita, M. Sano, Y. Hayakawa, H. Honjo, and Y. Sawada, Phys. Rev. Lett. **53**, 286 (1984).
[5] L. Paterson, Phys. Rev. Lett. **52**, 1621 (1984).
[6] P.G. Saffman and G.I. Taylor, Proc. R. Soc. London, Ser. A **245**, 312 (1958).
[7] M.B. Hastings and L.S. Levitov, Physica D **116**, 244 (1998).
[8] M.B. Hastings, Phys. Rev. E **55**, 135 (1997).
[9] B. Davidovitch, H.G.E. Hentschel, Z. Olami, I. Procaccia, L.M. Sander, and E. Somfai, Phys. Rev. E **59**, 1368 (1999).
[10] H.G.E. Hentschel and I. Procaccia, Physica D **8**, 435 (1983).
[11] T.C. Halsey, P. Meakin, and I. Procaccia, Phys. Rev. Lett. **56**, 854 (1986).
[12] T.C. Halsey, M.H. Jensen, L.P. Kadanoff, I. Procaccia, and B.I. Shraiman, Phys. Rev. A **33**, 1141 (1986).
[13] L.A. Turkevich and H. Scher, Phys. Rev. Lett. **55**, 1026 (1985).
[14] J. Klein and E. Kumacheva, J. Chem. Phys. **108**, 6996 (1998).
[15] E. Kumacheva and J. Klein, J. Chem. Phys. **108**, 7010 (1998).
[16] I. Tovstopyat-Nelip and H.G.E. Hentschel, Phys. Rev. E **61**, 3318 (2000).
[17] A. Marmur and M.D. Lelah, Chem. Eng. Commun. **13**, 133 (1981).
[18] F. Barra, B. Davidovitch, A. Levermann, and I. Procaccia, Phys. Rev. Lett. **87**, 134501 (2001).